

The Effect of Ferroelasticity of $\text{La}_{1-x}\text{Sr}_x\text{Co}_{1-y}\text{Fe}_y\text{O}_{3-\delta}$ on the Mechanical Stability of Solid Oxide Fuel Cells

Yuta Kimura^a, Julian Tolchard^b, Mari-Ann Einarsrud^b, Tor Grande^b, Koji Amezawa^c, Shin-ichi Hashimoto^d and Tatsuya Kawada^a

^a Graduate School of Environmental Studies, Tohoku University, 6-6-01 Aramaki-Aoba, Aoba-ku, Sendai 980-8579, Japan

^b Department of Materials Science and Engineering, Norwegian University of Science and Technology, 7491, Trondheim, Norway

^c IMRAM, Tohoku University, 2-1-1 Katahira, Aoba-ku, Sendai, 980-8577, Japan

^d Graduate School of Engineering, Tohoku University, 6-6-01 Aramaki-Aoba, Aoba-ku, Sendai 980-8579, Japan

The stress-strain relationship of $\text{La}_{0.6}\text{Sr}_{0.4}\text{CoO}_{3-\delta}$ (LSC), $\text{La}_{0.6}\text{Sr}_{0.4}\text{Co}_{0.2}\text{Fe}_{0.8}\text{O}_{3-\delta}$ (LSCF6428) and $\text{La}_{0.6}\text{Sr}_{0.4}\text{FeO}_{3-\delta}$ (LSF) was evaluated by uniaxial compression tests in the temperature range between room temperature and 1173 K. A nonlinear stress-strain relationship with a residual strain was observed below the phase transition temperature, while an almost linear relationship was with no residual strain was observed above the phase transition temperature. Cyclic tests revealed that the width of the hysteresis in the 2nd cycle was much smaller compared with that of the 1st cycle at room temperature. On the other hand, the difference in the stress-strain relationship and the effective compliance was hardly observed at 873 K. This result suggests that the apparent Young's modulus of the rhombohedral LSCF depends on the applied stress and the mechanical history due to ferroelasticity. Thus, the stress distribution in SOFCs can be affected by the ferroelasticity of LSCF.

Introduction

$\text{La}_{1-x}\text{Sr}_x\text{Co}_{1-y}\text{Fe}_y\text{O}_{3-\delta}$ (LSCF) is widely used as a cathode material for solid oxide fuel cells (SOFCs). TLSCF has a rhombohedral perovskite structure at low temperatures which transforms to a cubic structure at high temperatures (4-6). The phase transition temperature of LSCF increases with increasing iron content. The phase transition temperature of $\text{La}_{0.6}\text{Sr}_{0.4}\text{CoO}_{3-\delta}$ is reported to be about 753 K (4), while for $\text{La}_{0.6}\text{Sr}_{0.4}\text{Co}_{0.2}\text{Fe}_{0.8}\text{O}_{3-\delta}$ and $\text{La}_{0.6}\text{Sr}_{0.4}\text{FeO}_{3-\delta}$ values of 973-1073 K (5) and ~1073 K (6) are reported, respectively. The rhombohedral perovskite-type oxides are ferroelastic (10, 11) with four different domain orientations along $[111]$, $[1\bar{1}\bar{1}]$, $[\bar{1}11]$ or $[\bar{1}\bar{1}\bar{1}]$ direction (8, 9). When the rhombohedral LSCF material is exposed to a stress of a certain value, domains oriented in certain directions start switched to resulting in a non-linear stress-strain performance. Such a non-linear deformation may change the stress distribution in SOFCs especially during the starting up / shutting down process. Therefore, in order to precisely evaluate the stress distribution and determine the operational margin, it is

necessary to understand the ferroelastic behavior of LSCF. In this study, the stress-strain relationship of $\text{La}_{0.6}\text{Sr}_{0.4}\text{Co}_{1-y}\text{Fe}_y\text{O}_{3-\delta}$ (LSCF, LSC for $y = 0$, LSCF6428 for $y = 0.8$, LSF for $y = 1$) at high temperatures was investigated by uniaxial compression tests.

Experimental

Powders of LSCF6428 were purchased from AGC SEIMI CHEMICAL Co., Ltd. while powders of LSC and LSF were synthesized by the Pechini method. Nitrate solutions of La^{3+} , Sr^{2+} , Co^{3+} and Fe^{3+} , ethylene glycol and citric acid were mixed in an appropriate ratio, and heated to 673 K. The obtained polymeric precursor was calcined in air for 8 hours at 1248 K (LSC) or at 1373 K (LSF). The obtained powders of LSC and LSF and the powders of LSCF6428 were first compacted into cylinders by uniaxial pressing at about 10 MPa and then isostatically pressed at 150 MPa. The compacts were sintered in air for 6 hours at 1473 K (LSC), 1573 K (LSCF6428 and LSF) and slowly cooled with the rate of 106 K/h to avoid cracking. The sintered compacts of LSCF were machined into cylindrical samples of diameter 5.0-5.1 mm and height 9.5-10 mm. The surfaces of the samples were polished to a 1 μm finish. The deviation in parallelism of the surfaces was less than 10 μm . Relative densities of the samples were >95 %. The uniaxial compression tests were performed in the temperature range between room temperature and 1073 K in air. Details of the set-up are given elsewhere (12). A stress up to 300 MPa was applied by a 20 kN uniaxial actuator (Cormet digital control) and measured by 20 kN load cells (Cormet). The stress rate was ~ 25 MPa/min. The deformation of a sample was measured by an extensometer (MTS 634.31F-25 S/N 1144123). The sample was held 1 hour to attain equilibrium before each measurement. Once a measurement was performed, the sample was annealed at 1173 K for 1 hour. Then it was cooled and the next measurement was successively performed with the same sample.

Results and Discussion

Stress-strain relationship at various temperatures

Fig. 1 (a) shows the stress-strain relationship of LSCF6428 at room temperature in air. The stress-strain relationship under loading and unloading was irreversible and a residual strain was observed. Under loading, the relationship was almost linear at lower stress but above 70 MPa a clearly nonlinear behavior was observed. The relationship under unloading seemed to be more straight compared with that under loading but it was slightly nonlinear under lower stress. The effective compliance, S , of LSCF6428, which is the first derivative of the strain with respect to the stress under loading is also included in Fig. 1a. The effective compliance had a peak at about 140 MPa. Such a nonlinear stress-strain relationship with a residual strain and a peak in the effective compliance are also previously observed for LaCoO_3 and $\text{La}_{1-x}\text{Ca}_x\text{CoO}_3$ (12). At 473, 673 and 873 K (Fig. 1 (b)-(d)), the stress-strain relationship was nonlinear even starting from low stress levels. A residual strain was also observed at these temperatures but this residual strain was smaller compared to room temperature. The nonlinearity at lower stress under unloading becomes more significant compared with that at room temperature. At 473 K, a peak in the effective compliance was observed at about 20 MPa while at 673 and 873 K, the effective compliance only showed a comparatively high value at lower stress (less

than 50 MPa). At 1073 K (Fig. 1 (e)), the relationship under loading was almost linear up to about 250 MPa where a nonlinear behavior was observed. Contrary to the results below 873 K, the relationship under unloading was nonlinear when higher stress was applied and it became linear with decreasing the applied stress. A residual strain was also observed. The effective compliance was almost constant.

The nonlinear stress-strain relationship with a residual strain observed below 873 K can be associated with the ferroelasticity as the phase transition temperature of LSCF6428 is reported to be 973-1073 K (5). Below the phase transition temperature, LSCF6428 is rhombohedral (5) and cooling through the phase transition temperature during the cooling of the samples, randomly oriented domains are formed in the material. When sufficiently large stress is applied to the rhombohedral LSCF6428, domains with a proper orientation reorient to relax the stress. Considering the above, the stress-strain relationship of LSCF6428 below 873 K is expected to be as follows. When the applied stress is low, LSCF6428 deforms elastically and thus the relationship is linear. When the applied stress surpasses a critical stress, the domain switching gradually starts and the relationship becomes nonlinear. Simultaneously, the effective compliance becomes larger because the domain switching relaxes the applied stress. When further higher stress is applied, the domain switching begins to saturate and the effective compliance becomes smaller. After unloading, a residual strain is observed since the domain switching is irreversible. The nonlinearity under low stress can be associated with back switching of the domains. A peak in the effective compliance observed at room temperature and 473 K is considered to be due to the onset and the saturation of the domain switching. At 673 and 873 K, no peak was observed in the effective compliance but the compliance showed a large value at very low stress. This may be because the onset and the saturation of the domain switching occur at very low stress.

Since the phase transition of LSCF6428 from rhombohedral to cubic is a second-order phase transition, the crystal structure of LSCF6428 gradually changes from rhombohedral to cubic with increasing temperature (5). As the crystal structure approaches from rhombohedral to cubic, it is considered that the rhombohedral distortion becomes smaller and thus the strain which is introduced by the domain switching also becomes smaller. This can explain why the residual strain became smaller with increasing temperature.

Above 1073 K in air, LSCF6428 has a cubic crystal structure (5) and the material is paraelastic. Therefore, it is expected that the cubic LSCF6428 is elastic above 1073 K and the stress-strain relationship should be linear with no residual strain and the effective compliance is independent on the applied stress. However we observed creep deformation in the material at high loads giving the non-linear behavior at these stress levels. Lein *et al.* also reported creep deformation of LSCF at 1073 K (1).

An irreversible stress-strain relationship and a residual strain were also observed for LSC and LSF below 673 K (Figs. 2(a)-(c)) and 873 K (Figs. 3(a)-(c)), respectively. The relationship of both LSC and LSF was almost linear under both loading and unloading above these temperatures (Figs. 2(d)-(e) and Figs. 3(d)-(f)). The transition temperatures of LSC and LSF are reported to be 753 K (4) and 1073 K (6), respectively. Thus the limit temperatures at which the irreversible stress-strain relationship were observed agrees well with the phase transition temperatures of LSC and LSF. Above 1073 K, creep was also observed for both LSC and LSF.

LSCF deforms non-linearly due to ferroelasticity below the phase transition temperature. The critical stress for domain reorientation of LSCF becomes significantly smaller above 473 K and it is therefore possible that the non-linear deformation can occur

even when LSCF is exposed to very low stress in the temperature range between 473 and the phase transition temperature. Furthermore, creep deformation was observed above 1073 K. The stress distribution in SOFCs can be affected by these effects.

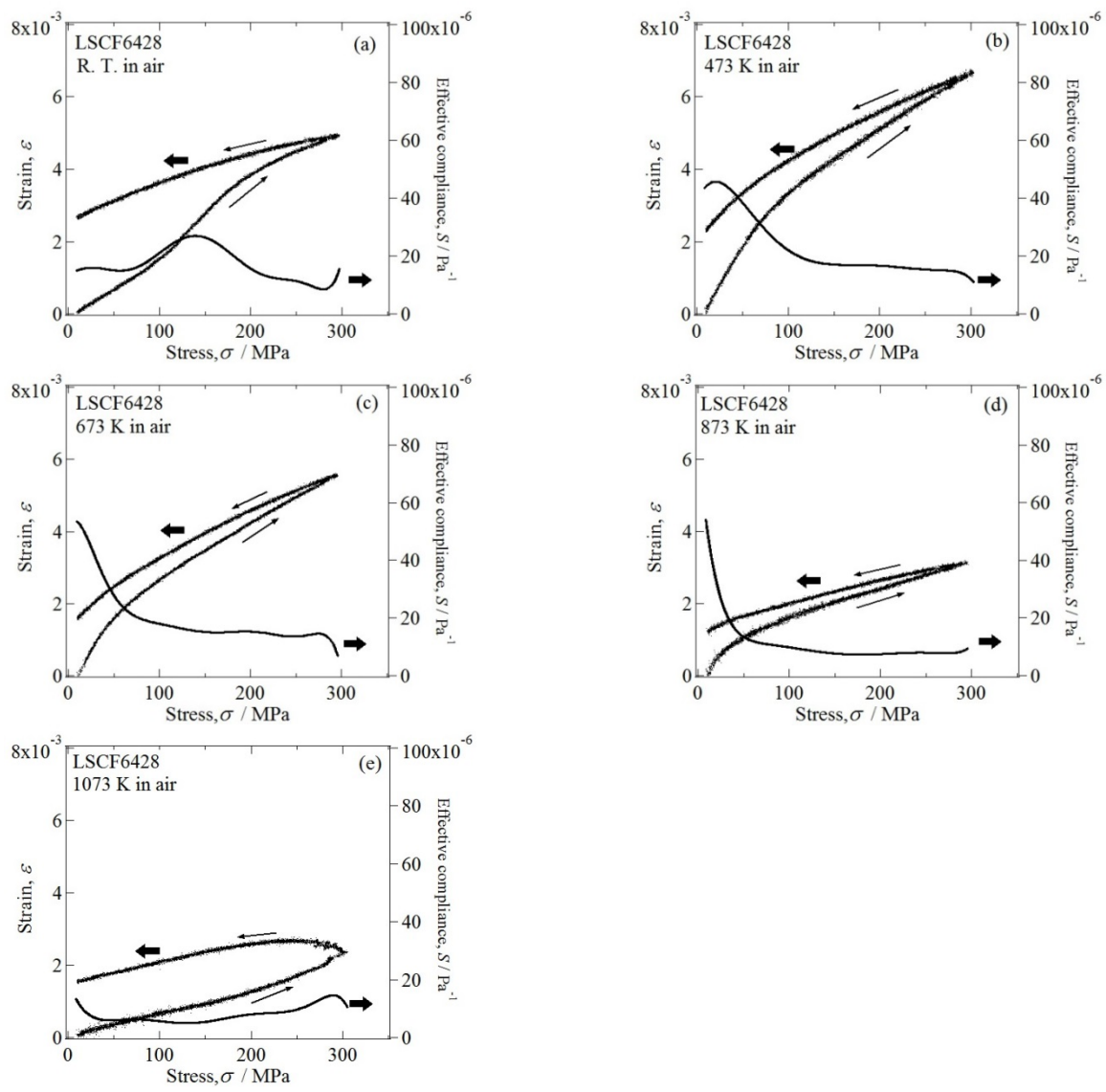


Fig. 1. Stress-strain relationship and the effective compliance of $\text{La}_{0.6}\text{Sr}_{0.4}\text{Co}_{0.2}\text{Fe}_{0.8}\text{O}_{3-\delta}$ (LSCF6428) under loading at various temperatures in air. (a) room temperature, (b) 473 K, (c) 673 K, (d) 873 K and (e) 1073 K. The solid line indicates the effective compliance.

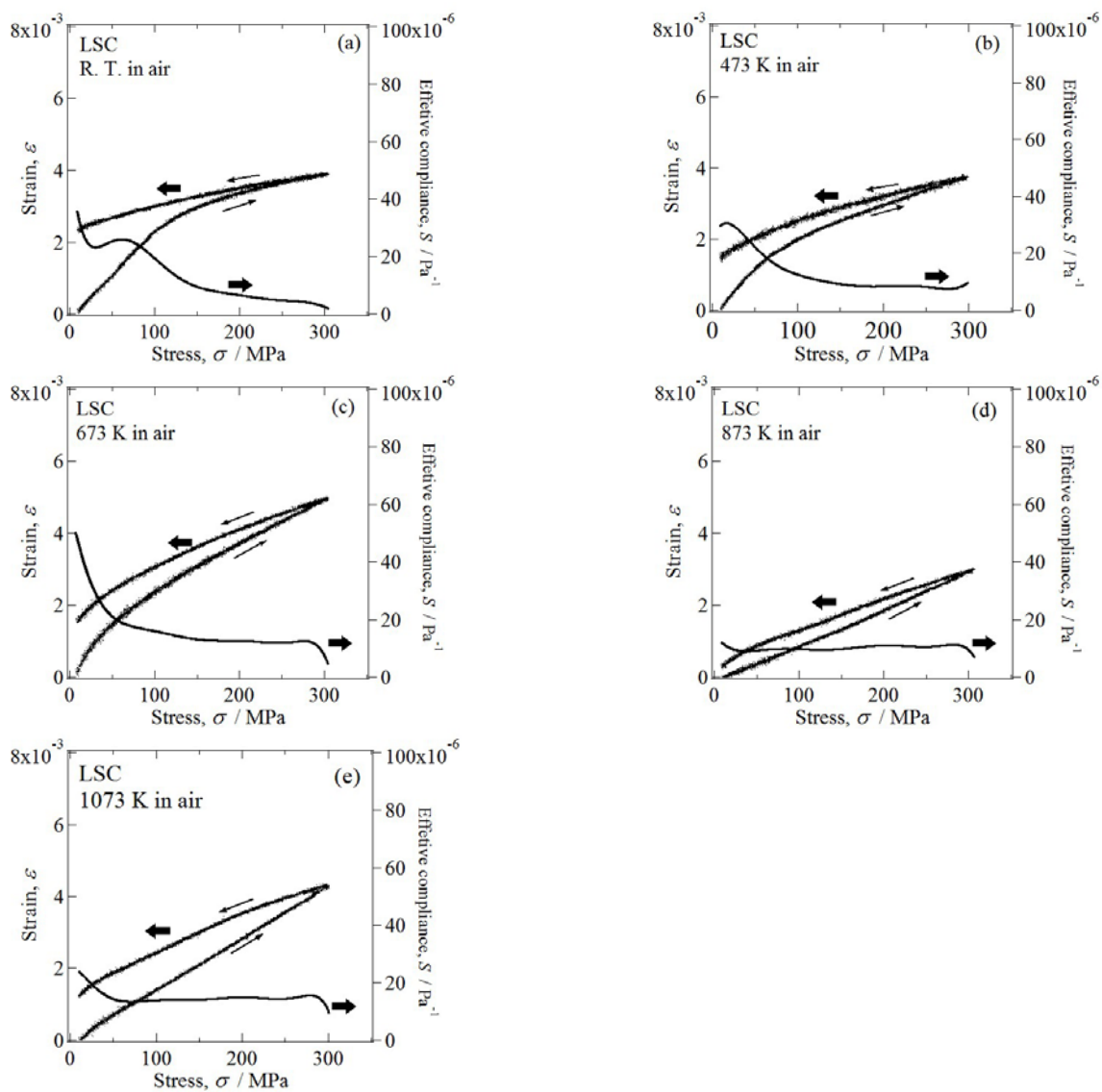


Fig. 2. Stress-strain relationship and the effective compliance of La_{0.6}Sr_{0.4}CoO_{3-δ} (LSC) under loading at various temperatures in air. (a) room temperature, (b) 473 K, (c) 673 K, (d) 873 K and (e) 1073 K. The solid line indicates the effective compliance.

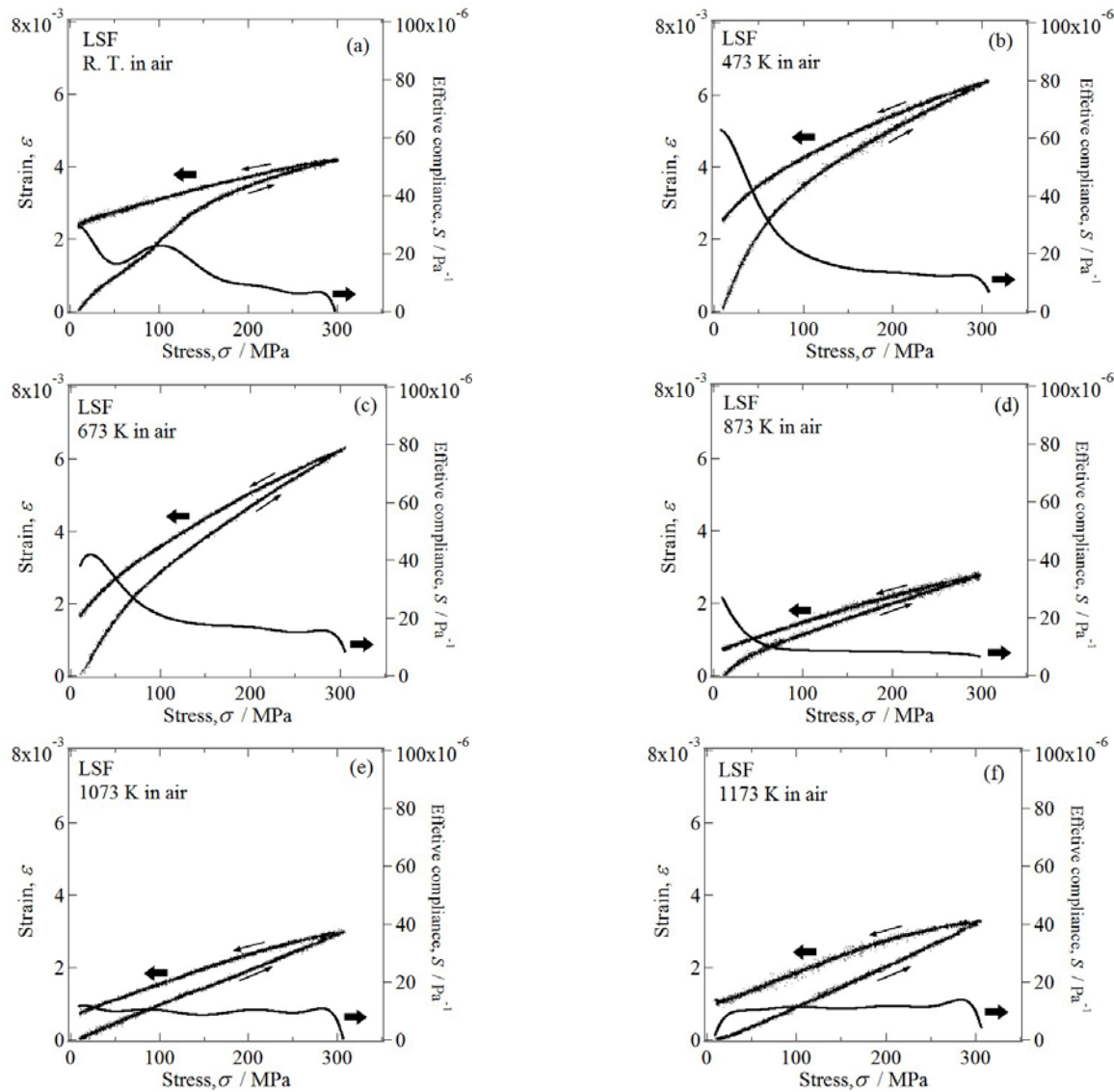


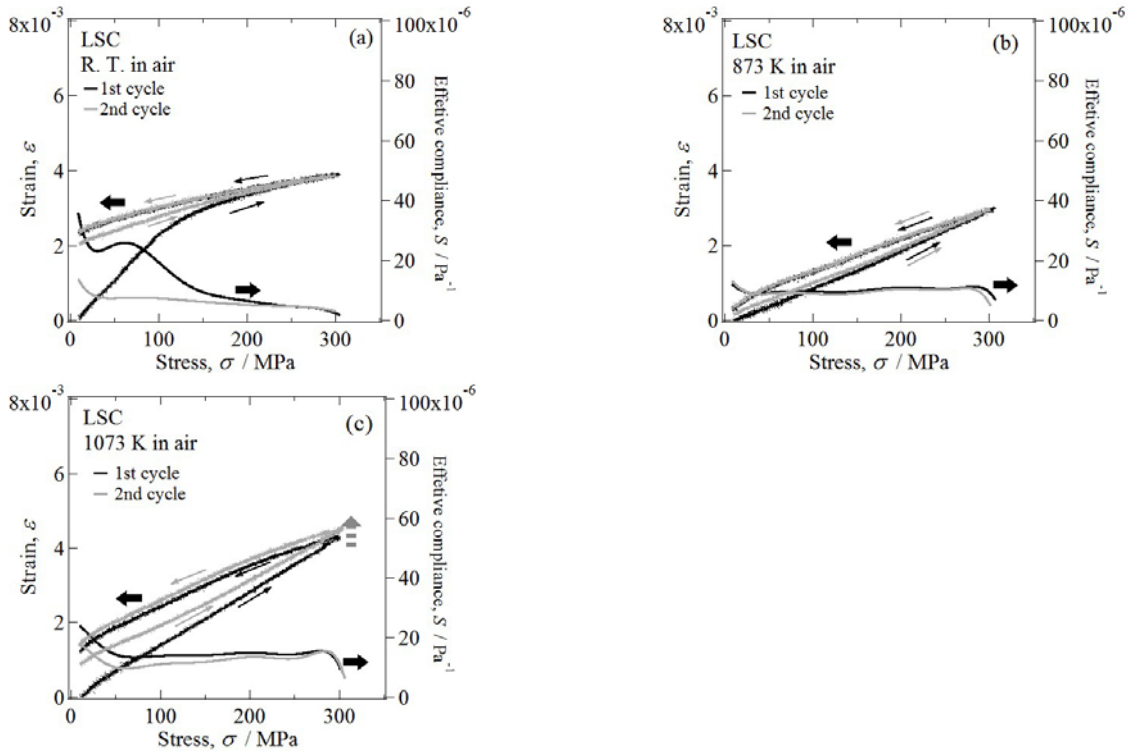
Fig. 3. Stress-strain relationship and the effective compliance of $\text{La}_{0.6}\text{Sr}_{0.4}\text{FeO}_{3-\delta}$ (LSF) under loading at various temperatures in air. (a) room temperature, (b) 473 K, (c) 673 K, (d) 873 K, (e) 1073 K and (f) 1173 K. The solid line indicates the effective compliance.

Cyclic tests of LSC

Figs. 4 (a)-(c) show the stress-strain relationship of LSC in loading-unloading cycles. The 1st and 2nd cycles were subsequently repeated without annealing the sample. At room temperature, the initial strain of the 2nd cycle was almost the same as the residual strain after the 1st cycle (Figs. 4 (a)). The 2nd cycle gave the same strain at maximum load. The width of the hysteresis in the 2nd cycle was much smaller compared with that of the 1st cycle. The residual strain during the first cycle at room temperature is considered to be due to the domain switching. Since the domains after the 1st cycle were not randomly oriented, the number of domains that can switch during the 2nd cycle is smaller than that of the 1st cycle. This seems to be the reason for the narrower hysteresis of the 2nd cycle. This result suggests that the apparent Young's modulus of LSCF

depends on the applied stress and the mechanical history below the phase transition temperature.. At 873 K where LSC has a cubic crystal structure a nearly linear behavior (Figs. 4 (b)) is observed as expected.

At 1073 K, the 2nd cycle gave the larger strain at maximum load than that of the 1st cycle. This supports that the LSC experiences creep deformation at this temperature. The width of the hysteresis in 2nd cycle was smaller than that of the 1st cycle. Thus, the primary creep is considered to finish during the 1st cycle and the secondary creep started in the 2nd cycle.



Figs. 4 Stress-strain relationship of LSC in the cyclic tests at (a) room temperature, (b) 873 K and (c) 1073 K. 1st and 2nd cycles of loading and unloading were subsequently repeated without annealing the sample.

Conclusion

The stress-strain relationship of LSC, LSCF6428 and LSF was evaluated by uniaxial compression tests in the temperature range between room temperature and 1173 K. The nonlinear stress-strain relationship with a residual strain was observed below the phase transition temperature. On the other hand, the relationship was almost linear and almost no residual strain was observed above the phase transition temperature. Above 1073 K, the stress-strain relationship of LSCF seemed to be affected by the creep deformation. These results suggest that the stress-strain relationship of LSC, LSCF6428 and LSF is influenced by ferroelasticity below the phase transition temperature. The critical stress of LSCF became significantly smaller above 473 K. It is possible that non-linear deformation due to the ferroelasticity can occur even when LSCF is exposed to very low stress in the temperature range between 473 and the phase transition temperature. The cyclic tests revealed that the width of the hysteresis in the 2nd cycle was much smaller

compared with the one of the 1st cycle at room temperature. At 873 K, the difference in the stress-strain relationship and the effective compliance was hardly observed. At 1073 K, the width of the hysteresis in 2nd cycle was smaller than that of the 1st cycle. This is due to creep deformation. The apparent Young's modulus of LSCF is considered to depend on the applied stress and the mechanical history below the phase transition temperature. It is suggested that LSCF is not ideally elastic except in the narrow temperature range from the phase transition temperature to about 1073 K. Therefore, the stress distribution in SOFCs during operation or starting up / shutting down can be affected by above mentioned plastic deformation.

Acknowledgements

This investigation was supported by the New Energy and Industrial Technology development Organization (NEDO), Japan.

References

1. H. L. Lein, O. S. Andersen, P. E. Vullum, E. Lara-Curzio, R. Holmestad, M.-A. Einarsrud and T. Grande, *J. Solid State Electrochem.*, **10**, 635 (2006).
2. A. Julian, E. Juste, P.M. Geffroy, N. Tessier-Doyen, P. Del Gallo, N. Richet, T. Chartier, *J. Euro. Ceram. Soc.*, **29**, 2603 (2009).
3. B. X. Huang, J. Malzbender and R. W. Steinbrech, *J. Mater. Res.*, **26**, 1388 (2011).
4. J. Mastin, M.-A. Einarsrud and T. Grande, *Chem. Mater.*, **18**, 6047 (2006).
5. B. X. Huang, J. Malzbender, R. W. Steinbrech and L. Singheiser, *Solid State Ionics*, **180**, 241 (2009).
6. A. Fossdal, M. Menon, I. Wærnhus, K. Wiik, M.-A. Einarsrud and T. Grande, *J. Am. Ceram. Soc.*, **87**, 1952 (2004).
7. Y. Kimura, T. Kushi, S. Hashimoto, K. Amezawa, T. Kawada, *J. Am. Ceram. Soc.*, **95**, 2608 (2012).
8. C. H. Kim, J. W. Jang, S. Y. Cho, I. T. Kim, K. S. Hong, *Mater., Physica B*, **262**, 438 (1999).
9. C. H. Kim, S. Y. Cho, I. T. Kim, W. J. Cho, K. S. Hong, *Mater. Res. Bull.*, **36**, 1561 (2001).
10. P. E. Vullum, R. Holmestad, H. L. Lein, J. Mastin, M. – A. Einarsrud and T. Grande, *Adv. Mater.*, **19**, 4399 (2007).
11. W. Araki and J. Malzbender, *J. Euro. Ceram. Soc.*, **33**, 805 (2013).
12. S. Faaland, T. Grande, M.-A. Einarsrud, P. E. Vullum, R. Holmestad, *J. Am. Ceram. Soc.*, **88**, 726 (2005).
13. Yuta Kimura, J. Tolchard, M.-A. Einarsrud, T. Grande, K. Amezawa, M. Fukuhara, S. Hashimoto and T. Kawada, *Proc. 19th International Conference on Solid State Ionics*, to be published.